

## Photocatalytic degradation of Malachite Green using ZnO and ZnO-TiO<sub>2</sub> nanoparticles from aqueous solution

Hadi Baseri\* and Elahe Alizadeh

School of Chemistry, Damghan University, Damghan, Iran

Received: 2018-04-24

Accepted: 2018-07-26

Published: 2018-10-01

### ABSTRACT

Today, despite the increasing demands for the products of chemical industries and the related factories, the challenges of environmental pollution have not been improved and it is approaching a very dangerous stage. In this regard, the role of dyeing industries in contaminating the environment is undeniable. In this research, ZnO and ZnO-TiO<sub>2</sub> nanoparticles were synthesized by co-precipitation and sol-gel methods, respectively. The synthesized nanoparticles were characterized by XRD and FE-SEM techniques and their band gap energy were determined using the UV-Vis spectrum obtained from the suspension of nanoparticles. By using synthesized nanoparticles, degradation of malachite green under irradiation of the UV (A) -Visible mixture light from aqueous solution were evaluated and the effect of different parameters such as amount of photo catalyst, time of light irradiation and dose of H<sub>2</sub>O<sub>2</sub> has been studied. The destruction amount was determined by UV-Vis spectroscopy method. Based on the reported results, the maximum degradation efficiency of about 99% was obtained in the optimal values of experimental conditions.

**Keywords:** Color Contaminant; Malachite Green; Nanoparticles; Photo Catalyst; ZnO; ZnO-TiO<sub>2</sub>

© 2018 Published by Journal of Nanoanalysis.

### How to cite this article

Baseri H., Alizadeh E. Photocatalytic degradation of Malachite Green using ZnO and ZnO-TiO<sub>2</sub> nanoparticles from aqueous solution. J. Nanoanalysis., 2018; 5(4): 232-240. DOI: 10.22034/jna.2018.544275

## INTRODUCTION

In the recent decades, contaminated waters are one of the main problems in developing countries. Wastewater that contaminated with die chemical products is one of the major industrial water pollution sources [1]. Various industries such as textile, food, plastics and cosmetics use different types of dyestuffs which also appear in the wastewaters discharged from these industries. Usually, synthetic dyes are toxic and therefore they must be removed immediately from aquatic sources, and otherwise they will lead to bad effects on the individual health. For example of these chemical dies, malachite green (MG) is one of the most commonly dyes used for cotton, paper, silk and paints or printing inks. The chemical structure of MG is shown in Fig. 1.

\* Corresponding Author Email: [baseri@du.ac.ir](mailto:baseri@du.ac.ir)

Removing of MG from aqueous solutions is difficult, because it belongs to the same group of tri-phenyl-methane dyes and they have properties that make them difficult to remove from aqueous solution. Some important properties of MG were reported in literature such as teratogenic [2], carcinogenic [3] and reproductive abnormalities [4] which spanning its effect from various fish to mammals [5].

Treating of dye contaminated wastewater studied by different methods of adsorption [6-11], membrane processes [12-15], coagulation-precipitation [16-18], biological processes [19,20] and etc. These methods are usually non-destructive and they may generate secondary pollution, because of these methods dyes are not destroyed and they transferred to another phase. Therefore,

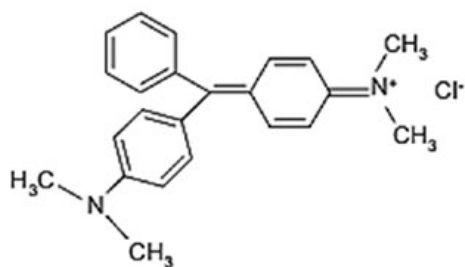


Fig.1. Chemical structure of Malachite Green (MG).

methods in which dye chemicals were destroyed are efficiently needed because they lead to degradation of toxic and refractory organics [21-29].

For removing chemical wastes from discharging wastewater, Nanomaterials proved to be useful and environmentally friendly candidates because they are easy to regenerate and are effective in dye removal from contaminated wastewater [30, 31]. In literature, different nanoparticles were successfully used to degrade dye compounds from aqueous solutions [32]. Nanoparticles like Titanium dioxide, Cupper oxide, Zinc oxide, Silver oxide and etc, were used widely by different researchers [33-36].

Zinc Oxide based composites exhibits different band gaps and they are being used by different research groups for degradation of organic dyes [37]. All of them use ultraviolet or visible light as a source of energy to create an electron hole pair for dye degradation.

In our present research pure nano ZnO and ZnO-TiO<sub>2</sub> nanoparticles were fabricated and the photocatalytic ability of these nanoparticles was studied. Moreover, the effects of some important effective parameters on the degradation efficiency were reported.

## MATERIAL AND METHODS

### Reagents

Analytical grade of chemicals was used in all of experiments. Titanium Isopropoxide (C<sub>12</sub>H<sub>28</sub>O<sub>4</sub>Ti with 97% purity and Mw=284.22 g/mol), Hydrated Zinc Nitrate (Zn(NO<sub>3</sub>)<sub>2</sub>.6H<sub>2</sub>O with 99% purity and Mw=297.49), Sodium Hydroxide (99% Purity), Hydrogen Peroxide (H<sub>2</sub>O<sub>2</sub>, 30% purity) and Malachite Green (C<sub>23</sub>H<sub>15</sub>ClN<sub>2</sub> with 99% purity and Mw=364/9 g/mol) were purchased from Merck (Germany). Ethanol (C<sub>2</sub>H<sub>5</sub>OH with purity of 99/5%), Hydrochloric Acid (HCl with 37% purity) and other used solvents were purchased from Sigma-Aldrich (Germany). Double distilled water (DW) is used in all experiments.

## EXPERIMENTAL PROCEDURES

### Production of Nano ZnO

ZnO nanoparticles were produced by coprecipitation method in which, 1 mole of Hydrated Zinc Nitrate is dissolved in 100 ml deionized water and Sodium Hydroxide solution was added to the first solution draperies with continued mixing until pH=12. The precipitated white powder was collected and washed three times with deionized water and then it dried in 90°C oven for 26 hours. Finally, the produced powder calcined in 500°C for 1 hour.

### Production of Nano composite of ZnO-TiO<sub>2</sub>

To prepare ZnO-TiO<sub>2</sub> nano composite, at first, 5 ml of TTIP was added to ethanol and mixed for about 1 hour with a magnetic sitter until a clear solution was produced. Then deionized water and HCl solution were added to first solution and mixed vigorously until clear and yellow solution of TiO<sub>2</sub> were formed. The solution of Zinc Nitrate – Ethanol was added to TiO<sub>2</sub> solution very slowly and the mixture was mixed continuously in the room temperature for 2 hours. The produced solution dried in 60°C for 20 hours and 110°C for 2 hours. Finally, to prepare a crystalline structure, the produced powder was calcined in 400°C for 3 hours.

### Material Characterization

To study the degree of crystallinity, structure and characteristics of the synthesized ZnO and ZnO-TiO<sub>2</sub> nanoparticles XRD, FE SEM and UV-Visible spectroscopy analyses have been performed.

X-ray diffraction (XRD) pattern of the produced particles was performed in a Bruker X-ray powder diffractometer (XRD, Rigaku smart lab, Cu K α1, Rigaku, Japan). All samples were swept from 2θ =10° to 80° with a speed of 1°/min.

Spectroscopic measurements of the synthesized nanomaterials were studied using a HITACHI (S-4160) field electron scanning microscope with maximum voltage of 30 KV and different magnitude of 20X to 30000X. In order to prevent charging, these samples were coated with carbon.

The UV-visible spectroscopy experiments were conducted on a Perkin Elmer (lambda 25) with a Peltier temperature programmer and a water bath (Lab Teach LCB).

### Photocatalytic degradation method

To study on the degradation of MG, different

values of synthesized nanocatalyst (0.01, 0.02, 0.03 and 0.04 g) is added to 25 ml of water-MG solution with concentration of 3 ppm. The mixture is continuously mixed by a magnetic heater stirrer for about 30 min in the light irradiation. A mercury vapor pressure lamp (250W) is used for its light source. The used lamp is a cheap and commercial light source which irradiates in UV & Vis spectrum range. This lamp emits about 90% of its power in visible regime and 10% of its power in ultra-visible regime ( $\lambda < 400$  nm). Finally, the powder solid catalyst is separated from the solution by centrifuging (4000 RPM & 20 min) and the remained concentration of MG in the solution is measured by UV-Vis spectroscopy. For the measurements, the calibration curves were plotted and degradation percent is calculated by the following formula:

$$\text{degradation percent} = \frac{C_0 - C_t}{C_0} \times 100 \quad (1)$$

In this equation  $C_0$  and  $C_t$  are the initial and final concentration of MG in the solution (ppm).

In this work various effective parameters (catalyst concentration, reaction time and H<sub>2</sub>O<sub>2</sub> concentration) on the MG degradation were studied for two synthesized nanocatalysts of ZnO and ZnO-TiO<sub>2</sub>. For studying on the effects of each parameter, the values of other parameters were remained constant in its optimum value.

## RESULT AND DISCUSSION

### Characterization of nanocatalysts

#### XRD analysis results

The crystalline structures of synthesized

nanocatalysts recognized with XRD patterns (Fig. 2). The X-ray diffraction pattern of synthesized TiO<sub>2</sub> nanoparticles shows that TiO<sub>2</sub> was successfully constructed. The  $2\theta$  at peak 25.4° confirms the TiO<sub>2</sub> anatase structure. Strong diffraction peaks at 25° and 48° indicating TiO<sub>2</sub> in the anatase phase. For ZnO nanoparticles, Sharpe peaks located at typical  $2\theta$  angles about 32, 35, 37, 47, 56, 64 and 68° show that ZnO was successfully synthesized and crystallized. The XRD patterns of ZnO are closely same of the pure ZnO powders reported in literature without any impurity peak; therefore produced ZnO have a wurtzite hexagonal phase [38].

For ZnO-TiO<sub>2</sub>, the values of  $2\theta$  ranges obtained in the spectrum corresponded to the reference pattern of ZnO-TiO<sub>2</sub> nanoparticles. According to this pattern, zinc oxide and titanium oxide are both synthesized. The crystallite sizes of the catalysts were calculated using the Scherrer's formula (Eq.2) [39]:

$$D = \frac{K\lambda}{\beta \cos \theta} \quad (2)$$

Where  $D$  is taken as average crystallite size,  $\lambda$  is 1.5406 Å,  $K$  is a constant equals to 0.9,  $\beta$  is the full width at half maximum (FWHM) in radians on the  $2\theta$  scale and  $\theta$  is Bragg angle for the diffraction peaks. According to the above equation, the average crystallite size of the synthesized TiO<sub>2</sub>, ZnO and ZnO-TiO<sub>2</sub> nanoparticles was estimated to be 21.5, 29.26 and 26.08 nm, respectively. The presence of TiO<sub>2</sub> has a characteristic effect on the particles size of the sample. This reduction is due to increased surface energy of ZnO-TiO<sub>2</sub> nanoparticles.

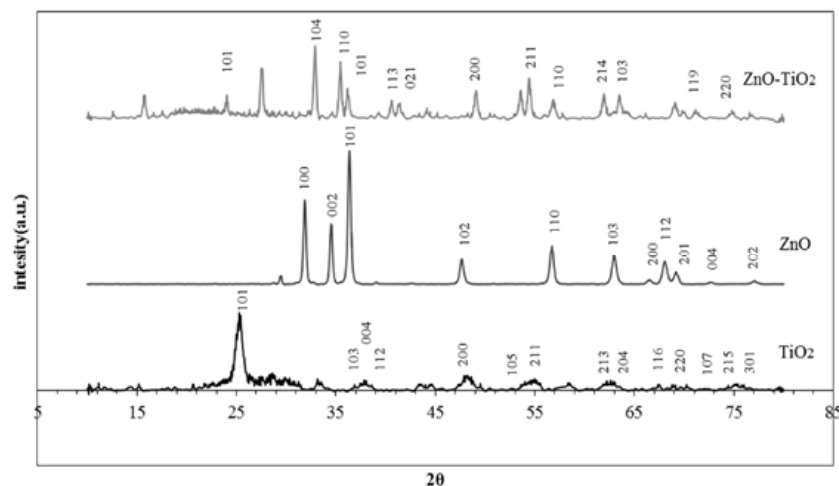


Fig. 2. XRD pattern of nano ZnO, TiO<sub>2</sub> and ZnO-TiO<sub>2</sub>

*FE-SEM analysis results*

FE-SEM image of ZnO and ZnO-TiO<sub>2</sub> nanoparticles are shown in Figs. 3 and 4, respectively.

The results of these images clearly show that by forming of ZnO-TiO<sub>2</sub> nano composite, the morphology and size of ZnO nanoparticles were changed completely.

Particle size distribution his to grams of ZnO and ZnO-TiO<sub>2</sub> nanoparticles are shown in Fig.5 and 6, respectively. As noted above, synthesized composite nanoparticles are smaller in size than Zinc Oxide nanoparticles, which are well illustrated in the diagrams below. The average area and diameter of obtaining nanoparticles are reported in Table 1.

*Study of optical properties of synthesized nanoparticles*

The absorption spectra of ZnO and ZnO-TiO<sub>2</sub>, is shown in Fig. 7. The energy band gap for samples was calculated by Eq (3) [40]:

$$E_g = \frac{hc}{\lambda} \quad (3)$$

Where *h* is Planck constant (*h*= 4.14×10<sup>-15</sup> ev.s), *c* is the speed of light (*c*= 2.99×10<sup>8</sup> m/s) and *λ* is wavelength of nanoparticles.

The band gaps of the nanoparticles were estimated 3.66 eV and 3.39 eV for ZnO and ZnO-TiO<sub>2</sub>, respectively. It's predicted that by decreasing of the band gap, the catalytic activity is increased.

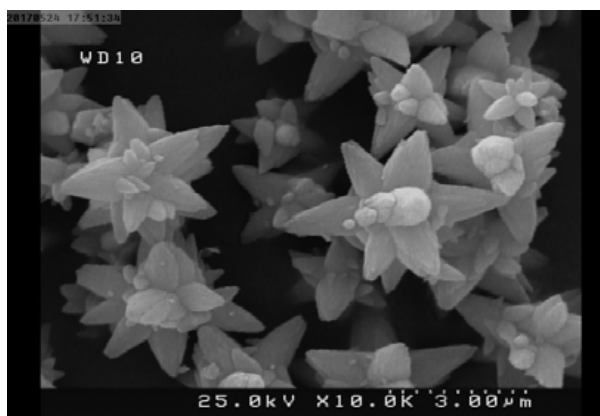


Fig.3. FE-SEM image of nano ZnO.

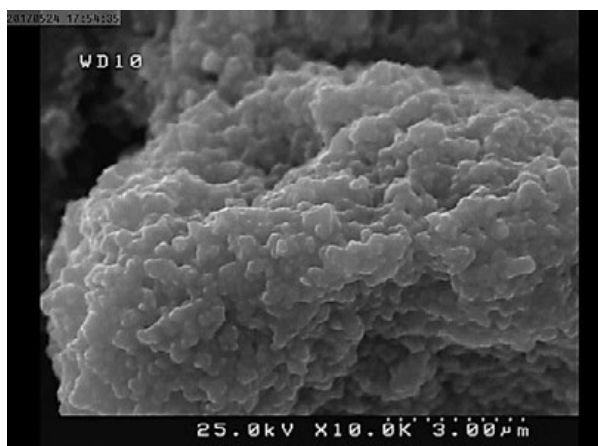


Fig. 4. FE-SEM image of nano ZnO-TiO<sub>2</sub>.

Table 1. Area and diameter of the synthesized nanoparticles

sample	ZnO	ZnO-TiO <sub>2</sub>
Average area (nm <sup>2</sup> )	8015.291	7247.262
Average diameter (nm)	101.05	96.08

*Effect of Photocatalysts dose on degradation of malachite green*

Fig. 8, shows the effect of ZnO photocatalyst dose on degradation of malachite green. The degradation reaction was carried out with different doses of photocatalysts. Various values of photocatalyst weight in the reaction medium (0.01, 0.02, 0.03 and 0.04 g) were examined. According to the results reported in this figure the optimal photocatalyst weight was 0.03 g with 44% destruction and this optimum value was used in all other experiments.

*The effect of time of light irradiation on degradation of malachite green*

In this section, the effect of visible light irradiation for removal of MG was examined. For this purpose, different radiation times were evaluated. A mercury vapor pressure lamp (250 W) is used for light source and the samples located in about 30 cm from the light source with continuous

stirring. The results are shown in Fig.9. As shown in this figure, with increasing of the irradiation time, the degradation of MG increased and ZnO-TiO<sub>2</sub> composite nanoparticles exhibit a better effect on the MG photocatalytic degradation. MG destroyed about 66% in 60 min Vis light irradiation.

*The effect of H<sub>2</sub>O<sub>2</sub> dose on degradation of malachite green*

These experiments were carried out in the presence of 0.03 g photocatalysts and 60 minutes of visible light irradiation. This effect is shown in Fig.10. Like the reported results in other papers [41], with increasing the dose of H<sub>2</sub>O<sub>2</sub>, removal efficiency increased [2, 41]. The accepted mechanism for the photolysis of H<sub>2</sub>O<sub>2</sub> is the cleavage of the molecule into hydroxyl radicals, which are very strong oxidizing types. These radicals can oxidize organic compounds (RH) producing organic radicals (R<sup>o</sup>), which are highly reactive and can undergo further

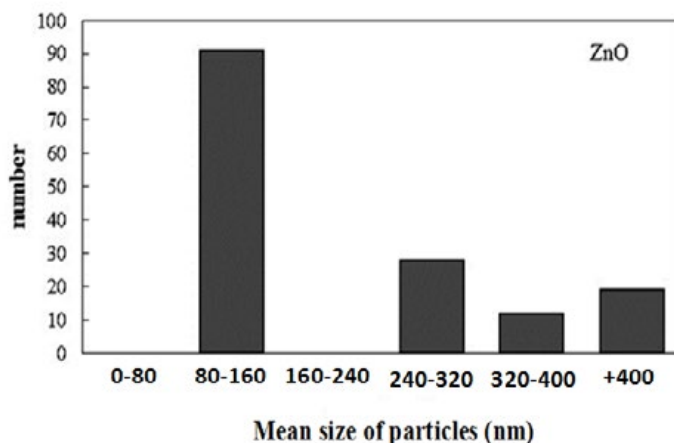


Fig. 5. Obtained Histogram from FE-SEM images of nano ZnO.

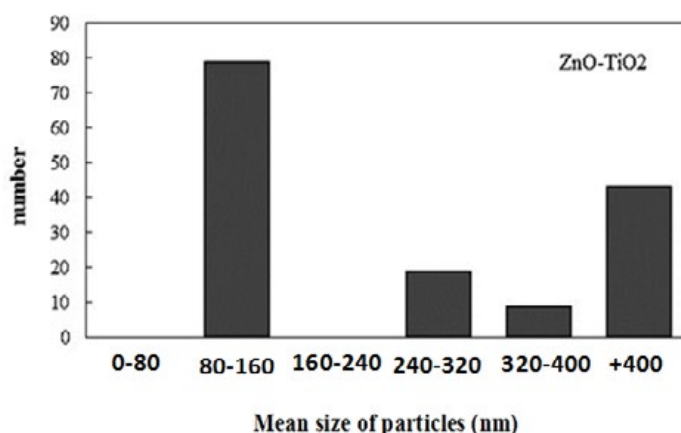


Fig. 6. Obtained Histogram from FE-SEM images of nano ZnO-TiO<sub>2</sub>.

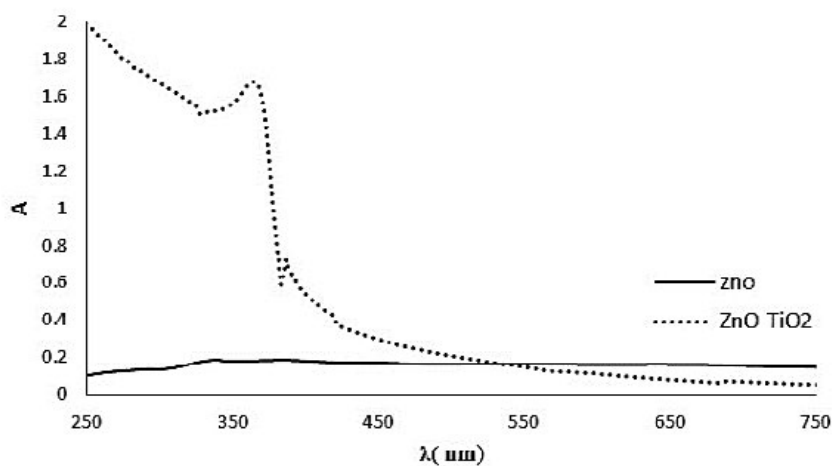


Fig. 7. UV-Vis diffuse reflectance spectra.

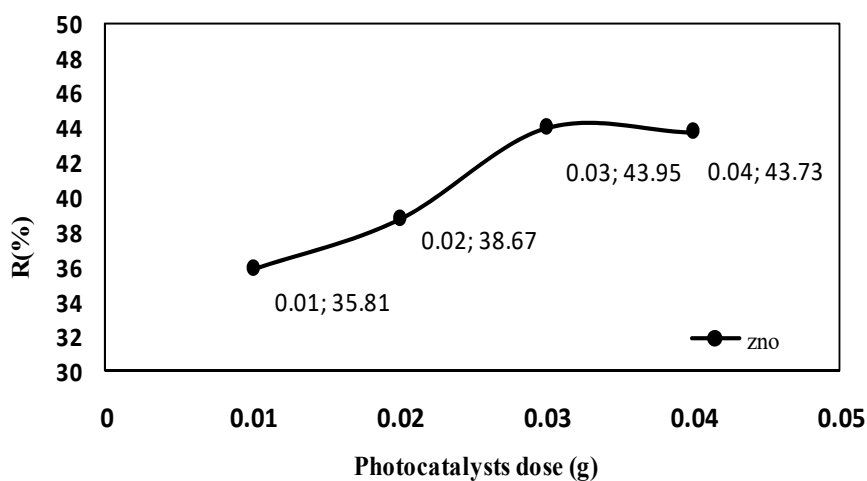


Fig. 8. Effect of photocatalysts dose on the removal of MG.

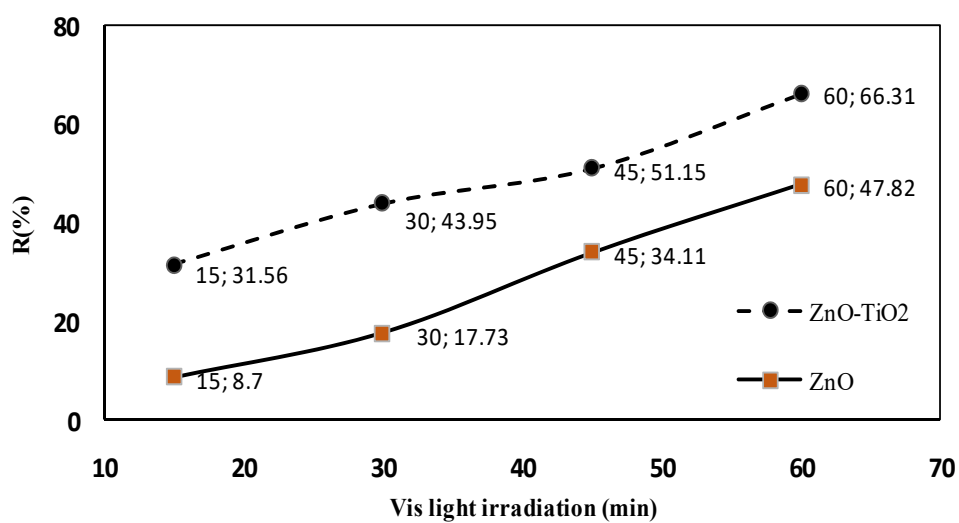
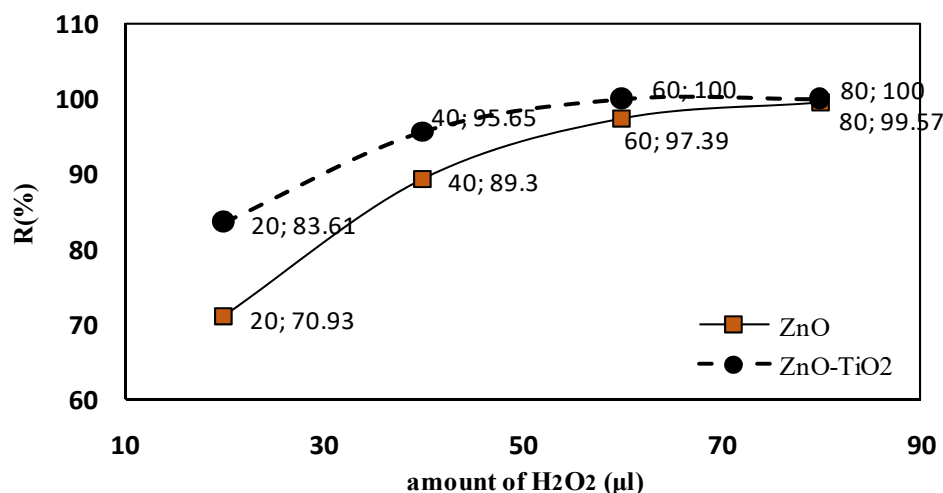
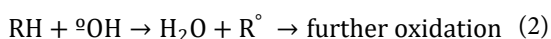


Fig. 9. The effect of time of visible light irradiation on the removal of MG.

Fig. 10. Effect of H<sub>2</sub>O<sub>2</sub> dose on the removal of MG.

oxidation. The possible reactions, which occur during process, are as follows:



If the operation is carried out under suitable conditions, the final products are H<sub>2</sub>O, CO<sub>2</sub> and low molecular weight aliphatic acids [42].

## CONCLUSION

More than 10,000 different types of synthetic dyes are produced and used in various industries in all over the world. Their waste products contain significant amounts of dye organic compounds that create irreparable damage in the environment. Therefore, the treatment of dye wastewater is necessary before it is discharged into the environment. Today, removing these contaminants using nanoparticles is a very simple, low-cost, and efficient way. The Malachite Green is one of the pollutants used both in dyeing industry and as a medicine for fish breeding. The results showed that ZnO and ZnO-TiO<sub>2</sub> nanoparticles could be prepared successfully. The use of both photocatalytic synthesized in nanoscale has shown very good results in removing the MG. The results of photocatalytic experiments showed that in the absence of an oxidant, the optimal photocatalyst value is 0.03 g and the time of visible light irradiation is 60 minutes. In this condition, about 66% of malachite green was removed from aqueous solution using ZnO-TiO<sub>2</sub> photocatalysts

but in the presence amount of oxidizing agents, the decolorization process was completed.

## CONFLICT OF INTEREST

The authors declare that there is no conflict of interests regarding the publication of this manuscript.

## REFERENCES

- 1.T. R. Bastami and A. Ahmadvour, Preparation of magnetic photocatalyst nano hybrid decorated by poly oxometalate for the degradation of a pharmaceutical pollutant under solar light. *Environ. Sci. Pollut. Res.*, 23, 8849(2016).
- 2.S.J. Culp, L.R. Blankenship, D.F. Kusewitt, D.R. Doerge, L.T. Mulligan and F.A. Beland, Toxicity and metabolism of malachite green and leucomalachite green during short-term feeding to Fischer 344 rats and B6C3F<sub>1</sub> mice, *Chem. Biol. Interact.*, 122, 247(1999).
- 3.K. Lee, J. Wu and Z. Cai, Determination of malachite green and leucomalachite green in edible goldfish muscle by liquid chromatography-ion trap mass spectrometry, *J. Chromatogr. B.*, 843, 247 (2006).
- 4.C. Cha, D.R. Doerge and C.E. Cerniglia, Biotransformation of Malachite Green by the Fungus *Cunninghamella elegans*, *Appl. Environ. Microbiol.*, 67, 4358(2001).
5. S. Srivastava, R. Sinha and D. Roy, Toxicological effects of malachite green, *Aquat. Toxicol.*, 66, 319 (2004).
- 6.M. Rajabi, B. Mirza, K. Mahanpoor, M. Mirjalili, F. Najafi, O. Moradi, H. Sadegh, R. Shahryari-ghoshekandi, M. Asif, I. Tyagi, S. Agarwal and V. K.Gupta, Adsorption of malachite green from aqueous solution by carboxylate group functionalized multi-walled carbon nanotubes: determination of equilibrium and kinetics parameters, *J. Ind. Eng. Chem.*, 34, 130 (2016).
- 7.R. Elmoubarki, F.Z. Mahjoubi, H. Tounsadi, J. Moustadraf, M. Abdennouri, A. Zouhri, A. El Albani and N. Barka,

- Adsorption of textile dyes on raw and decanted Moroccan clays: Kinetics, equilibrium and thermodynamics, *Water Resour. Inst.*, 9, 16 (2015).
8. N. Barka, S. Qourzal, A. Assabbane, A. Nounah and Y. Ait-Ichou, Removal of Reactive Yellow 84 from aqueous solutions by adsorption onto hydroxyapatite, *J. Saudi Chem. Soc.*, 15, 263 (2011).
  9. H. Tounsadi, A. Khalidi, M. Abdennouri and N. Barka, Biosorption potential of *Diplotaxis harra* and *Glebionis coronaria* L. biomasses for the removal of Cd (II) and Co (II) from aqueous solutions, *J. Environ. Chem. Eng.*, 3, 822 (2015).
  10. C. Djilani, R. Zaghoudi, F. Djazi, B. Bouchekima, A. Lallam, A. Modarressi and M. Rogalski, Adsorption of dyes on activated carbon prepared from apricot stones and commercial activated carbon, *J. Taiwan Inst. Chem. Eng.*, 53, 112 (2015).
  11. O. Njoku, K.Y. Foo, M. Asif and B.H. Hameed, Preparation of activated carbons from rambutan (*Nephelium lappaceum*) peel by microwave-induced KOH activation for acid yellow 17 dye adsorption, *Chem. Eng. J.*, 250, 198 (2014).
  12. A.J. Kajekar, B.M. Dodamani, A.M. Isloor, A.K. Zulhairun, N.B. Cheer, A.F. Ismail and S.J. Shilton, Preparation and characterization of novel PSf/PVP/PANI-nanofiber nanocomposite hollow fiber ultrafiltration membranes and their possible applications for hazardous dye rejection, *Desalination*, 365, 117 (2015).
  13. X. Chen, Y. Zhao, J. Moutinho, J. Shao, A.L. Zydney and Y. He, Recovery of small dye molecules from aqueous solutions using charged ultrafiltration membranes, *J. Hazard. Mater.*, 284, 58 (2015).
  14. T. Chidambaram, Y. Oren and M. Noel, Fouling of nanofiltration membranes by dyes during brine recovery from textile dye bath wastewater, *Chem. Eng. J.*, 262, 156 (2015).
  15. J. Lin, W. Ye, H. Zeng, H. Yang, J. Shen, S. Darvish manesh, P. Luis, A. Sotto and B. Van der Bruggen, Fractionation of direct dyes and salts in aqueous solution using loose nanofiltration membranes, *J. Membr. Sci.*, 477, 183 (2015).
  16. A.K. Verma, R.R. Dash and P. Bhunia, A review on chemical coagulation/flocculation technologies for removal of colour from textile wastewaters, *J. Environ. Manag.*, 93, 154 (2012).
  17. S. Sadri Moghaddam, M.R. Alavi Moghaddam and M. Arami, Coagulation/flocculation process for dye removal using sludge from water treatment plant: optimization through response surface methodology, *J. Hazard. Mater.*, 175, 651 (2010).
  18. F.R. Furlan, L. Graziela de Melo da Silva, A.F. Morgado, A. Augusto Ulson de Souza and S.M.G. Ulson de Souza, Removal of reactive dyes from aqueous solutions using combined coagulation/flocculation and adsorption on activated carbon, *Resour. Conserv. Recycle.*, 54, 283 (2010).
  19. B. Bonakdar pour, I. Vyrides and D.C. Stuckey, Comparison of the performance of one stage and two stage sequential anaerobic-aerobic biological processes for the treatment of reactive-azo-dye-containing synthetic wastewaters, *Int. Biodeterior. Biodegrad.*, 65, 591 (2011).
  20. A.R. Khataee, G. Dehghan, A. Ebadi, M. Zarei and M. Pourhassan, Biological treatment of a dye solution by Macroalgae *Chara* sp.: Effect of operational parameters, intermediates identification and artificial neural network modeling, *Bioresour. Technol.*, 101, 2252 (2010).
  21. N. Barka, S. Qourzal, A. Assabbane, A. Nounah and Y. Ait-Ichou, Photocatalytic degradation of an azo reactive dye, Reactive Yellow 84, in water using an industrial titanium dioxide coated media, *Arab. J. Chem.*, 3, 279 (2010).
  22. N. Barka, S. Qourzal, A. Assabbane, A. Nounah and Y. Ait-Ichou, Photocatalytic degradation of patent blue V by supported TiO<sub>2</sub>: Kinetics, mineralization, and reaction pathway, *Chem. Eng. Commun.*, 198, 1233 (2011).
  23. M. Abdennouri, M. Baâlala, A. Galadi, M. El Makhfouk, M. Bensitel, K. Nohair, M. Sadiq, A. Boussaoud and N. Barka, Photocatalytic degradation of pesticides by titanium dioxide and titanium pillared purified clays, *Arab. J. Chem.*, (in press).
  24. M. Abdennouri, A. Galadi, N. Barka, M. Baâlala, K. Nohair, M. Elkrati, M. Sadiq and M. Bensitel, Synthesis, characterization and photocatalytic activity by par-chlorotoluene photooxidation of tin oxide films deposited on Pyrex glass substrates, *Phys Chem. News.*, 54, 126 (2010).
  25. K. Ayoub, E.D. Hullebusch, M. Cassir and A. Bermond, Application of advanced oxidation processes for TNT removal: a review, *J. Hazard. Mater.*, 178, 10 (2010).
  26. A.M. Asiri, M.S. Al-Amoudi, T.A. Al-Talhi and A.D. Al-Talhi, Photodegradation of Rhodamine 6G and phenol red by nanosized TiO<sub>2</sub> under solar irradiation, *J. Saudi Chem. Soc.*, 15, 121 (2011).
  27. B.A. Wols and C.H.M. Hofman-Caris, Review of photochemical reaction constants of organic micropollutants required for UV advanced oxidation processes in water, *Water Res.*, 46, 2815 (2012).
  28. S. Saha and A. Pal, Microporous assembly of MnO<sub>2</sub> nanosheets for malachite green degradation, *Sep. Purif. Technol.*, 134, 26 (2014).
  29. E.S. Baeissa, Photocatalytic degradation of malachite green dye using Au/NaNbO<sub>3</sub> nanoparticles, *J. Alloy. Compd.*, 672, 564 (2016).
  30. C. Bouasla, M.E. Samar and F. Ismail, Degradation of methyl violet 6B dye by the Fenton process, *Desalination*, 254, 35 (2010).
  31. S. He, G.S. Wang, C. Lu, X. Luo, B. Wen, L. Guo and M.S. Cao, Controllable fabrication of CuS hierarchical nanostructures and their optical, photocatalytic, and wave absorption properties, *Chem. Plus. Chem.*, 78, 250 (2013).
  32. D. Mohan and C.U. Pittman Jr, Arsenic removal from water/wastewater using adsorbents—a critical review, *J. Hazard. Mater.*, 142, 1 (2007).
  33. M. Rana, H.J. Cho, T.K. Roy, L.M. Mirica, and A.K. Sharma, Azo-dyes based small bifunctional molecules for metal chelation and controlling amyloid formation, *Inorganica, Chimica, Acta.*, 471, 419 (2018).
  34. X. Chen, D. Chu, L. Wang, W. Hu, H. Yang, J. Sun, and S. Zhang, Hydrogen peroxide-assisted synthesis of novel three-dimensional octagonal-like CuO nanostructures with

- enhanced visible-light-driven photocatalytic activity, *J. Mol. Struct.*, 1157, 337 (2018).
35. N. Boussatha, M. Gilliot, H. Ghoualem and J. Martin, Formation of nanogranular ZnO ultrathin films and estimation of their performance for photocatalytic degradation of amoxicillin antibiotic, *Mater. Res. Bull.*, 99, 485 (2018).
36. C. Jaramillo-Páez, J.A. Navío and M.C. Hidalgo, Silver-modified ZnO highly UV-photoactive, *J. Photochem. Photobiol. A.*, 356, 112(2018).
37. A. Modwi, M.A. Abbo, E.A. Hassan, O.K. Al-Duaij and A. Houas, Adsorption kinetics and photocatalytic degradation of malachite green (MG) via Cu/ZnO nanocomposites, *J. Environ. Chem. Eng.* 5, 5954(2017).
38. D. Jung, Syntheses and characterizations of transition metal-doped ZnO, *Solid State Sci.*, 12, 466 (2010).
39. M. Forouzani, H. R. Mardani, M. Ziari, A. Malekzadeh and P. Biparva, Comparative study of oxidation of benzyl alcohol: influence of Cu-doped metal cation on nano ZnO catalytic activity, *Chem. Eng. J.*, 275, 220 (2015).
40. E.S. Baeissa, Photocatalytic degradation of malachite green dye using Au/NaNbO<sub>3</sub> nanoparticles, *J. Alloy. Compd.*, 672, 564 (2016).
41. C. Galindo, P. Jacques and A. Kalt, Photochemical and photocatalytic degradation of an indigoid dye: a case study of acid blue 74 (AB74), *J. Photochem. Photobiol. A.*, 141.1, 47 (2001).
42. M.A. Behnajady, N. Modirshahla, M. Mirzamohammady, B. Vahid and B. Behnajady, Increasing photoactivity of titanium dioxide immobilized on glass plate with optimization of heat attachment method parameters, *J. Hazard. Mater.*, 160, 508 (2008).